# Comparing Centrifuge, Steady-State and Semi-Dynamic Methods for Relative Permeability and Capillary Pressure Determination: New Insights

*Fabrice* Pairoys[1,*], *Cyril* Caubit[1], *Micah* Alexander[2], and *Javier* Ramos[2]

[1]TOTAL CSTJF, Pau, France
[2]Schlumberger Reservoir Laboratories, Houston, United States

**Abstract.** Relative permeability and capillary pressure are essential parameters for understanding multiphase flow in porous media and scenarios of production in oil or gas reservoirs. There are several experimental methods for determining the relative permeability curves: unsteady-state (USS), steady-state (SS), and semi-dynamic (SD) methods. Each method has advantages and weaknesses. Although the USS approach leads to fast data results, the interpretation neglects the capillary pressure effects and provides a limited amount of data points obtained after breakthrough. The SS method is time consuming but enables covering a wider range of saturation with data points if the test is well designed. The SD method may be more time consuming than the SS method but provides both relative permeability to the injected phase and capillary pressure. The relative permeability to the produced phase is then determined by numerical means. The main objective of this study was to compare the water-oil relative permeability curves obtained from the steady-state and semi-dynamic methods performed at reservoir conditions with live fluids. Carbonate core plugs of same rock type and same properties were selected for this experimental program. The samples were brought to the same irreducible water saturation at a constant brine-oil capillary pressure using a centrifuge before being dynamically aged with live oil. In addition to monitoring the average saturation using material balance (MB), a linear X-ray scanner was used for in-situ saturation monitoring (ISSM) along the core samples. The oil relative permeability from the SD method was simulated with fixed water relative permeability and capillary pressure by history-matching the oil production and the differential pressure signal. Two additional centrifuge tests on twin plug were performed in order to measure imbibition capillary pressure and oil relative permeability at pseudo-reservoir conditions. This comparative study shows that the SD method provides similar capillary pressure and oil relative permeability curves to those obtained by centrifuge methods. Even if all Kr curves are in an acceptable envelop, some differences are observed between SD and SS Kr curves: several investigative leads are given to explain this discrepancy. It is also shown that a better saturation method needs to be implemented, especially when dealing with heterogeneous rocks. While a more robust ISSM method is being tested at TOTAL, the results presented in this paper are very encouraging.

## 1 Introduction

Relative permeability and capillary pressure are important petrophysical parameters for interpreting fluid flow in reservoirs and for calibrating appropriate reservoir simulation models. They are obtained in the laboratory, separately in most of the cases. The only method able to dynamically measure both parameters on a same test is the semi-dynamic method. This method was first implemented by [1]. By recirculating the produced fluid at constant pressure at the outlet of rock sample, the capillary pressure Pc at the core inlet is directly equal to the differential pressure dP, assuming the outlet capillary pressure is nil. The injected fluid relative permeability $Kr_{inj}$ can be obtained from the slope of the injected fluid rate Qi plotted against the inlet Pc (or dP). The inlet injected phase analytical saturation given by [1] has a similar form to that of Welge equation. With this method, relationships for relative permeability of the injected phase and capillary pressure are obtained.

Using the semi-dynamic approach, [2] developed a method to provide both positive and negative Pc for drainage and imbibition cycles at ambient conditions, using an ultrasonic method for monitoring the local saturation. Later, the same method was validated and used by [3] to build an integrated petrophysical tool able to determine full Pc curves, resistivity index and end-point relative permeability at reservoir conditions. [4] used the technique for measuring full Pc curves with live fluids at reservoir conditions. Relative permeabilities were derived by history matching of the transient pressures and saturation profiles acquired by X-ray attenuation method. [5] studied the variability in Pc curves due to local

* Corresponding author: fabrice.pairoys@total.com

© The Authors, published by EDP Sciences. This is an open access article distributed under the terms of the Creative Commons Attribution License 4.0 (http://creativecommons.org/licenses/by/4.0/).

heterogeneity using the semi-dynamic method with x-ray in situ saturation monitoring. [6] and [7] used the method at reservoir conditions with x-ray saturation monitoring for estimating oil recovery from transition zones. More recently, [8] developed a full petrophysical rock characterization workflow similar to [3] but included the full relative permeability curve, the produced phase relative permeability being derived from the electrical properties or using history match process. Few other studies can be found in the literature, there is not one comparing the semi-dynamic capillary pressure Pc and relative permeability Kr to those obtained from the standard methods, centrifuge and steady-state methods. The aim of the study is to compare data results from all these methods, performed at true reservoir conditions with live fluids (except for centrifuge tests). A 1D linear x-ray scanner was used to monitor the saturation profiles obtained at capillary equilibrium. It is shown that a more robust in situ saturation monitoring method is required to avoid erroneous interpretation, especially for heterogeneous rocks.

## 2 Background

The steady-state method is well known and accepted in the industry for determining relative permeability, it is not really the case for the semi-dynamic method despite being investigated since the '90s. A description of the method is found in [1]. The main idea is to recirculate the produced fluid at constant pressure at the outlet of the rock while injecting the displacing fluid at several constant rates at the inlet until steady-state condition (no more variation of saturation and differential pressure). In the following, consider an imbibition cycle, water displacing oil.
The method allows obtaining the relative permeability of the injected water phase, Krw, the analytical water saturation, Sw, and the capillary pressure, Pc, at the inlet of the core. It is a unique way of determining both Kr and Pc during a single coreflooding test.

A set of pressure drops, final average saturations and flow rates are required inputs for the method which consists of three steps:

1- The capillary pressure at the inlet simply equals the pressure drop (with oil gradient pressure and outlet Pc equal to 0):

$$Pc = dP = P_i(inlet) - P_o(outlet) \quad (1)$$

2- The relative permeability of water at the inlet of the sample is calculated using Darcy's law:

$$Krw = \frac{\mu_w L}{k_{eo}(Swi)A}\frac{dQ_w}{dPc} \quad (2)$$

The relative permeability to oil Kro, with fixed relative permeability to water and capillary pressure, is then determined by numerical simulation and history match of the oil production volume, Vo, and differential pressure dP

3- The oil saturation at the inlet is calculated by differentiating the product of steady-state water Darcy velocity and average oil saturation, leading to the following simplified equation:

$$So = < So > + Q_w \frac{d<So>}{dQ_w} \quad (3)$$

and

$$Sw = 1 - So = 1 - \left( < So > + Q_w \frac{d<So>}{dQ_w} \right) \quad (4)$$

Equation 4 can be substituted with a direct measurement of the inlet saturation using in situ saturation monitoring such as x-ray method.

## 3 Rocks and Fluids

In this study, a tight carbonate rock was selected. Several core plugs were extracted from a same whole core to perform composite stack coreflooding experiments, semi-dynamic and steady-state tests, and also centrifuge tests, with the aim of comparing the methods for Kr and Pc characterization. The core plug selection was based on the degree of heterogeneity of the samples, using CT scan images. All fractured core plugs were discarded.

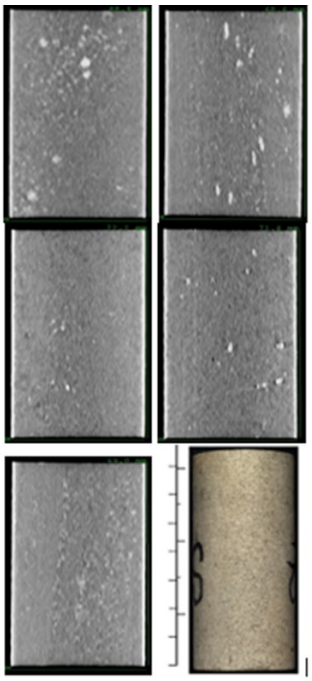

**Fig. 1.** CT scan images of samples S1/S2 (SDM), S3/S4 (SS), S5 (Centrifuge) and 1 core plug photography of sample S1

There were no miscible tracer tests programmed in this study. However, it is highly recommended to perform these tests to discard the rocks with too high longitudinal heterogeneity (especially for the unsteady-state experiments) but also to compare the degree of heterogeneity from one rock to another one.

XRD was performed on the end-trims to confirm the selected core plugs had the same mineralogy. The clay-free samples represent limestones composed of 90-95% calcite with traces of anhydrite, potassium feldspar and quartz. Before measuring the porosity and permeability, the core plugs were batch-cleaned in Soxhlet using a chloroform/methanol azeotropic mixture and then dried in a convection oven at 116°C. The routine properties were measured at 2000 psi of net confining stress (NCS), representative of the NCS applied during the coreflooding

and centrifuge tests. Table 1 proves that the samples have similar properties.

**Table 1.** Routine core properties

| Plug Id | Test Type | He ϕ (%) | Kg (mD) | Kw (mD) |
|---|---|---|---|---|
| S1 | SD | 12.7 | 1.35 | 0.75 |
| S2 | SD | 12.1 | 1.25 | 0.51 |
| S3 | SS | 15.6 | 2.09 | 0.92 |
| S4 | SS | 14.7 | 1.21 | 0.63 |
| S5 | Pc centri | 16.1 | 1.78 | 0.66 |

The core plugs were individually saturated with a 220 kppm synthetic formation brine before being desaturated with dead oil. A recombined oil was also prepared to replace the dead oil before performing the coreflooding experiments with live fluids. Fluid properties at various experimental conditions are listed in Table 2:

**Table 2.** Fluid properties

| | Pp (psig) | T (°C) | $\rho_w$ (g/cc) | $\rho_o$ (g/cc) | $\mu_w$ (cP) | $\mu_o$ (cP) |
|---|---|---|---|---|---|---|
| SD&SS | 3000 | 100 | x | x | 0.48 | 3.17 |
| Centrifuge | 0 | 70 | 1.12 | 0.85 | 0.66 | 5.45 |

Both brine and oil were filtered through a 0.1 µm filter to limit potential plugging issues during the tests (based on MICP pore throat size distribution).

Figure 2 shows pore throat radius going down to 0.05µm, highlighting the necessity of the 0.1µm fluid filtering process. The distribution looks unimodal but spread along the pore throat radius range. All selected samples have similar pore throat size distributions.

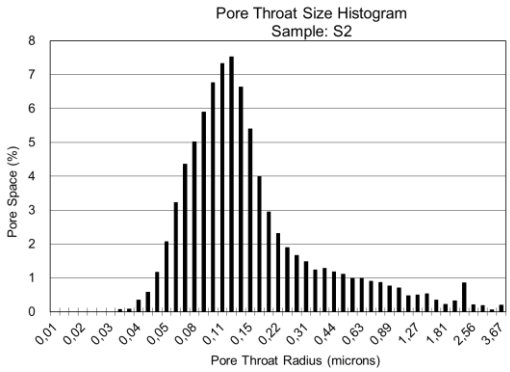


**Fig. 2.** MICP pore throat size distribution

Figure 3 represents an example of thin section (TS) and Scanning Electron Microscopy (SEM) images from S1 end-trims, confirming a certain degree of heterogeneity.

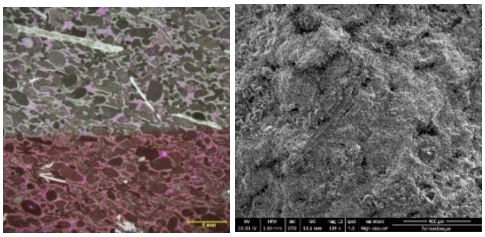

**Fig. 3.** TS and SEM images

## 4 Experimental Setups, Conditions and Methodology

The same coreflooding system was used to perform the SD and SS tests (Figure 4):

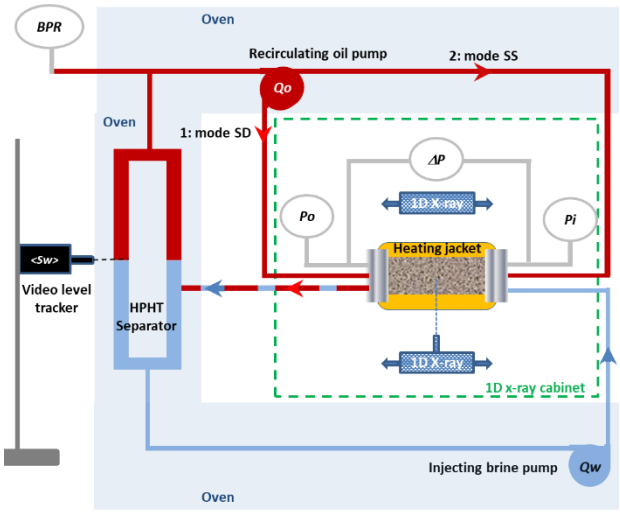


**Fig. 4.** Schematic of the HPHT coreflooding system

The coreflooding system is composed of a triple-pump system per phase -brine and oil- for injection and recirculation (mode 1 for SD method, mode 2 for SS method), an x-ray transparent core holder with heating jacket in x-ray protective cabinet, a 1D linear x-ray system for measuring saturation profiles, one High Pressure High Temperature (HPHT) video level tracker for material balance monitoring, three differential pressure sensors of different ranges with automatic switches, two -inlet and outlet- pressure transducers, a back pressure regulator with single pump pore pressure control, and one single pump controlling the confining pressure. All measurements are automatically recorded during the tests.

A centrifuge with ability to perform the tests under confining pressure was used to determine multispeed centrifuge Pc and single-step Kro tests. Note it is not possible to perform live oil experiments in a centrifuge (no pore pressure, limited temperature). In the centrifuge tests, NCS of 2000 psi was applied (Table 2).

After the 100% brine saturation under vacuum and applied hydrostatic pressure of 5000 psi, the samples were centrifuged at a constant capillary pressure Pc with dead oil up to irreducible water saturation Swi. To reduce the capillary end-effects, they were flipped to flatten the saturation profile during a second centrifuge step. The samples were then loaded in the x-ray transparent core holders (two composite stacks of two samples) and brought to the reservoir conditions (100 °C of temperature, 3000 psi of pore pressure Pp and 5000 psi of confining pressure Pconf. Samples with the lowest permeability were placed at the outlet of each composite stack. Stack 1 was composed of samples S1 and S2 for the SD test. Stack 2 was composed of samples S3 and S4 for the SS test. Sample S5 was loaded in a Hassler core holder and dynamically aged with dead oil for four weeks. S5 was then measured for effective permeability to oil at

irreducible water saturation, then loaded in a centrifuge core holder for the forced imbibition cycle (without spontaneous imbibition). After cleaning and measuring porosity and permeability properties to ensure the rock was not altered during the centrifuge multistep test and cleaning, the same sample was later aged again and tested for single-step centrifuge desaturation in order to calculate the relative permeability to oil.

Four weeks of dynamic aging was performed to restore the rock wettability. As for S5, the effective oil permeability Keo at Swi on the two stacks (stack 1 for SD and stack 2 for SS tests) was measured prior water flooding.

**Table 3.** Initial conditions

| Test Type | Sample Id | Oil Type | Keo (mD) | Swi (frac.) | X-Swi (frac.) |
|---|---|---|---|---|---|
| SD | S1/S2 | Live | 0.387 | 0.223 | 0.224 |
| SS | S3/S4 | Live | 0.385 | 0.193 | 0.188 |
| Centri Pc | S5 | Dead | 0.216 | 0.197 | x |
| Centri Kro | S5 | Dead | 0.196 | 0.203 | x |

The design of the SD and SS Kr coreflooding tests and multistep Pc and single-step Kro centrifuge tests was performed using the core analysis software CYDAR, using a first guess of Kr/Pc anticipating a slightly water-wet behaviour based on previous works.

## 5 Experimental Results

SD results on S1/S2:

Figure 5 represents the differential pressure and the oil production versus time acquired during the SD experiment:

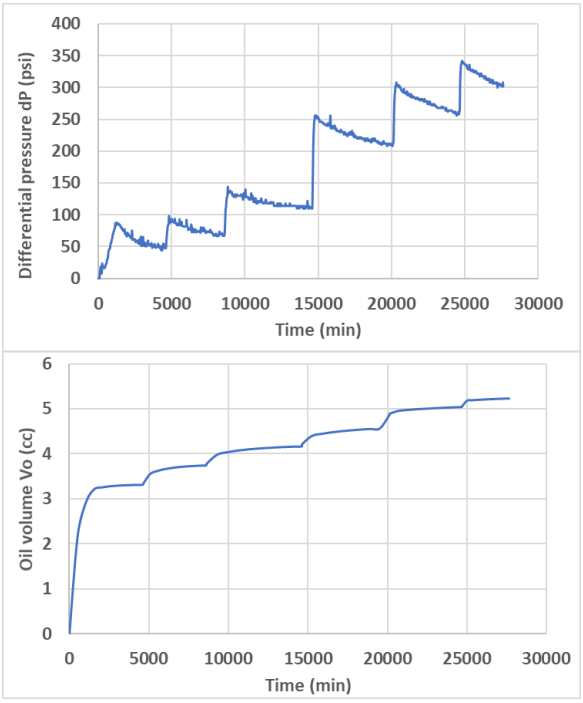


**Fig. 5.** dP and produced Vo versus time during the SD waterflood

The stabilization criteria were difficult to reach: if the stabilization criterion for oil production (<0.5% PV change in 24hr) was obtained, the dP stabilization was not fully satisfying, leading to a potential slight shift of the resulting Pc curve. Concerning the saturation profiles, the applied stabilization criterion was 10 overlapping and consecutive scans. This criterion was satisfied.

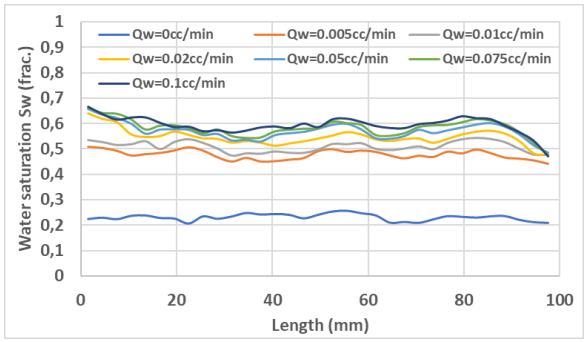


**Fig. 6.** Saturation profiles at equilibrium

To reduce the error on the counting, a minimum of 10,000 counts was successfully targeted, leading to less than 1% error on the number of transmitted photons (calculation via Poisson's law): it was achieved by applying a counting time per point of 5 seconds, at the specific applied energy.

The experimental design and specification limitations did not allow to obtain saturation profiles well spread on the full saturation range (Figure 6). The average of the water saturation profiles $<Sw_{x\text{-}ray}>$ obtained from x-ray attenuation technique and average water saturation $<Sw_{sep}>$ obtained from material balance using the separator at each stabilized step were found to be very close (<3 saturation units, s.u.), as shown on Figure 7:

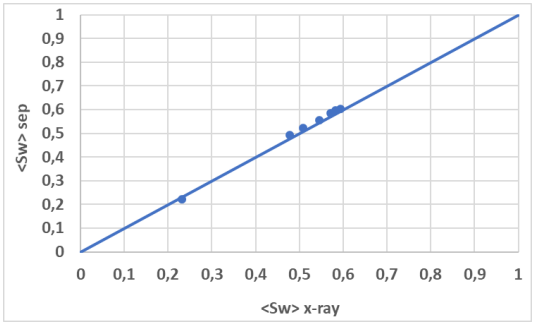


**Fig. 7.** Comparison between separator <Sw> and x-ray <Sw> during the SD waterflood

Figure 7 shows the robustness of both methods to acquire averaged saturations. On the other hand, higher discrepancy was observed between the analytical inlet local Sw calculation using Equation 4 and inlet local Sw value from the linear 1D x-ray method:

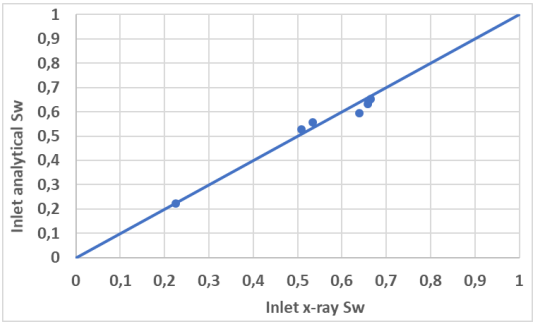


**Fig. 8.** Comparison between inlet local x-ray and analytical saturations at each equilibrium step

Although the comparative result looks acceptable, a single point of x-ray measurement does not allow to accurately capture the local saturation at the inlet section due to the degree of heterogeneity, the difference going up to 5 s.u. It is highly recommended for future tests to acquire more points on the full inlet section, requiring at least a 2D x-ray acquisition.

Nevertheless, the saturation profiles can help validate the numerical simulations and provide qualitative information on the rock wettability state.

Figure 9 represents the SD relative permeability curves on Cartesian and semi-log scale:

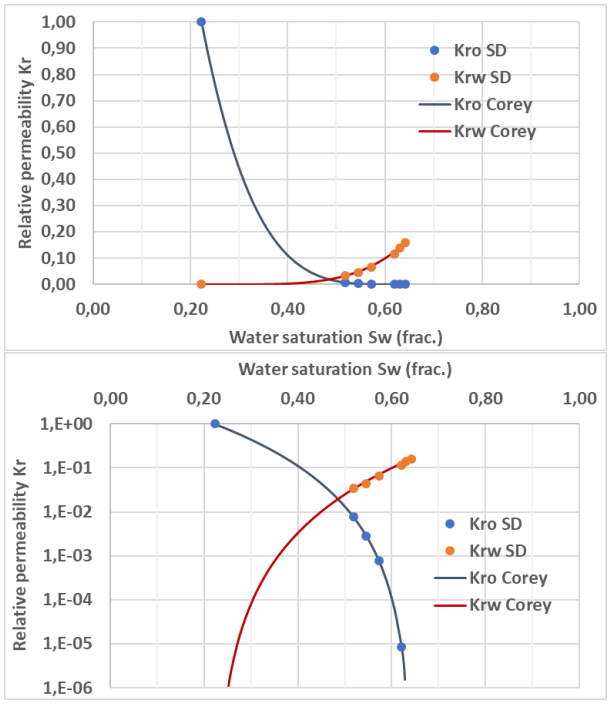


**Fig. 9.** SD Kr curves (Cartesian and semi-log plots)

Krw was directly obtained using Equation 2 while Kro was obtained by history matching oil production and differential pressure. The Sw values in Figure 9 are the ones analytically calculated using Equation 4, with <So> calculated using the produced oil volume from the separator. In the simulations, Pc was also entered using measured data points, fitted with a log(beta) function allowing positioning of the saturation Sw at Pc=0: this fitting function was optimized during the history-matching process.

The experimental program could not fully satisfy the CYDAR design due to too low water rate required to obtain Kr data points well spread over the saturation range, as shown in Figure 9. The minimum water rate applied during the test was 0.005 cc/min (lowest limit), the maximum rate was 0.1 cc/min (due to dP limitation).

To best fit the Kr data points, a Corey model was used. The values of the water and oil Corey exponents are:

Nw=4.5
No=4.0
Krw Max=0.16
Swi=0.224
Sor=0.346

The capillary pressure curve was directly obtained from the differential pressure values at each equilibrium, as explained in the background section. Figure 10 represents the measured differential pressure or capillary pressure versus Sw, with the fitting log(Beta) function used for the numerical simulations.

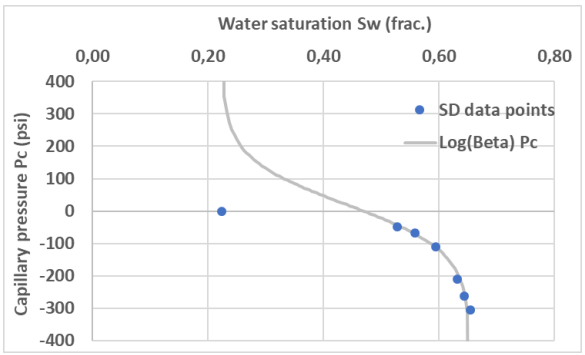


**Fig. 10.** SD Pc data points and optimized fitted Pc curve using a log(Beta) function

Unfortunately, the positive part of the Pc curve was not acquired for this project. A first attempt of fitting function going from Pc=0 at Swi value and passing through all data points using a single hyperbola function did not allow to match the oil production and differential pressure well. A log(Beta) function was used to fit the measured data points and to successfully history match the oil production and differential pressure. The data point at Pc=0 can be at a value of Sw varying from Swi to Sor. The saturation profiles were used to provide an estimation of this value (Sw=0.47 at Pc=0). The results of the numerical simulations and history matching are presented later.

The log(Beta) function is a 3 input-parameter function [Po, β, Sw(Pc=0)] in CYDAR, as defined in Equation 5:

$$Pc = cP_m \ln\frac{(1-Sw^{*B})}{Sw^{*B}} - b \qquad (5)$$

With Pm a pressure coefficient to control the magnitude of the Pc curve, Sw* the reduced saturation (Sw*=[Sw-Swi]/[1-Swi-Sor]), B coefficient to control the asymmetry of the function, b, a function dependent on the water saturation at Pc=0, and c parameter calculated as a function of β to impose a slope equal to Po at the middle of the Pc curve (Sw*=0.5). In the following simulations, the parameters Po and β were kept constant for both SD and SS numerical simulations: only the value of Sw(Pc=0)

was changed, according to the observation on the saturation profiles of the SD and SS tests.

**Table 4.** Parameters of the log(Beta) Pc function

| Tests | Po (bars) | β | Sw(Pc=0) |
|---|---|---|---|
| SD | 20 | 1 | 0.47 |
| SS | 20 | 1 | 0.57 |

SS results on S3/S4:

Figure 11 represents both dP and produced Vo versus time:

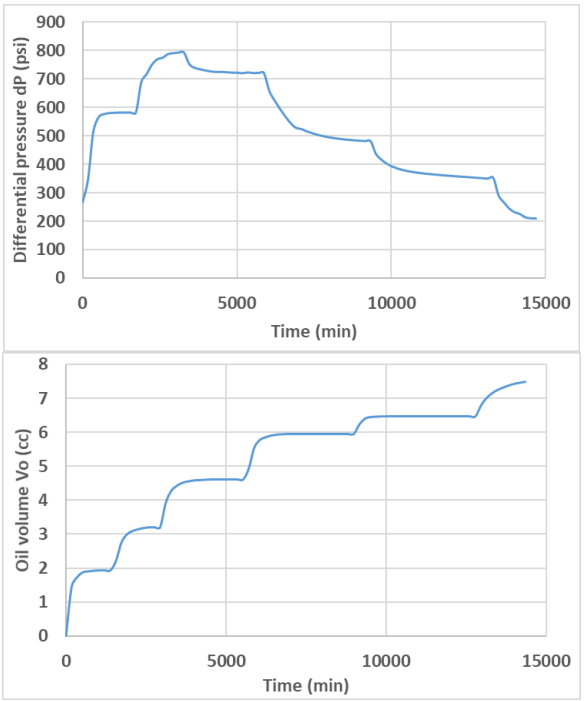


**Fig. 11.** dP and produced Vo versus time during the SS waterflood

For this test, the stabilization criteria were all obtained.

Concerning the saturation monitoring (Figure 12), the saturation profiles were noisier than the ones from the SD test: despite the choice of similar or "twin" samples and same experimental protocol, rocks may have different degree of heterogeneity.

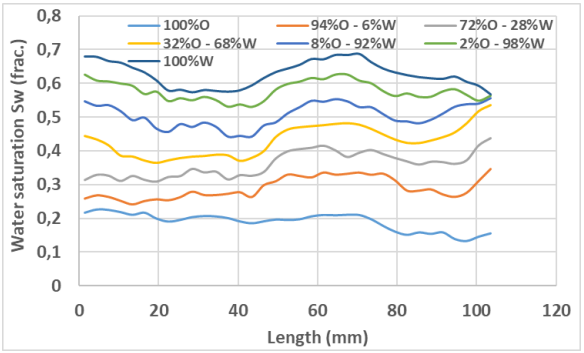


**Fig. 12.** Saturation profiles at equilibrium

Test parameters were well designed, with data points well spread over the saturation range. The outlet Sw seems to converge towards a value of 0.57. this information helps in choosing the imbibition log(beta) Pc curve for further numerical simulations.

Again, the comparison between the average water saturation <Sw> obtained by material balance and by averaging the x-ray profiles is acceptable, with less than 3 s.u. difference (Figure 13):

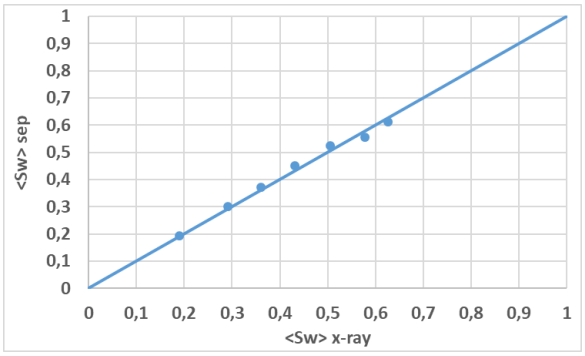


**Fig. 13.** Comparison between $<Sw_{sep}>$ and $<Sw_{x\text{-}ray}>$ during the SS waterflood

Figure 14 represents the non-interpreted SS relative permeability curves on Cartesian and semi-log scale:

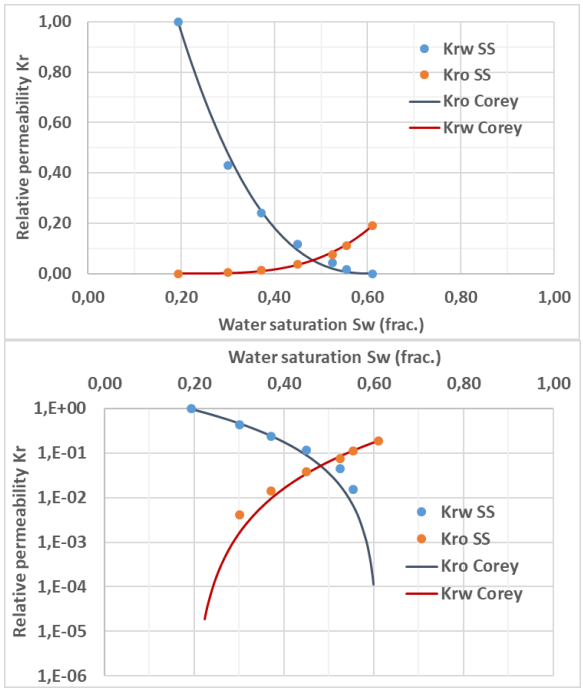


**Fig. 14.** SS Kr curves (Cartesian and semi-log plots)

The saturation Sw points are those calculated by material balance. Similar curve is obtained by using the average saturation profiles. As for the SD test, a Corey model was used to best fit the data points. The values of the water and oil Corey exponents are:

Nw=3.5
No=2.5
Krw Max=0.191
Swi=0.193
Sor=0.389

Pc centrifuge results on S5:

A forced imbibition multistep centrifuge test was performed to measure the capillary pressure Pc of sample S5. Unfortunately, there was no spontaneous imbibition performed before starting the forced imbibition. This step would have been interesting to compare with the value of SD Sw at Pc=0.

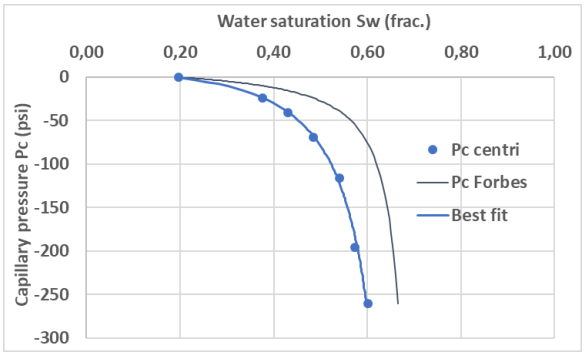


**Fig. 15.** Capillary pressure Pc (experimental and local Forbes Pc)

A modified hyperbolic function was first used to fit the experimental data points before calculating the local inlet saturation using Forbes' approach.

The same sample S5 was cleaned, brine-saturated, brought to Swi and run for single-step centrifuge (10000rpm) with dead oil to determine Kro. Note that intermediate porosity and permeability measurements were performed to ensure good sample integrity.

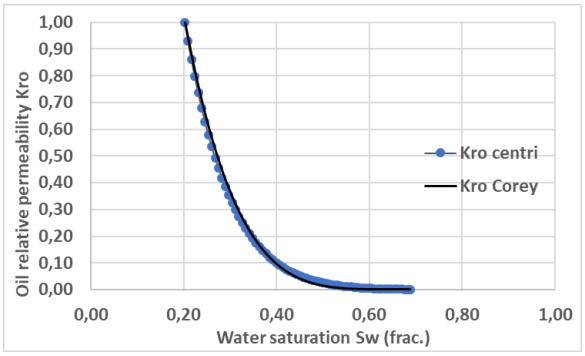


**Fig. 16.** Relative permeability to oil Kro from single-step centrifuge

Collected data were analysed using techniques published in [9] and [10], taking into account the correction for ramp up, capillary hold up, and mobility effects. The resulting oil relative permeability was then fitted with a Corey model. The No exponent was found to be equal to 4.0.

## Interpretation: Simulations and History Matching

### SD Method:

The results of the history-match process on the semi-dynamic waterflood are shown in Figure 17:

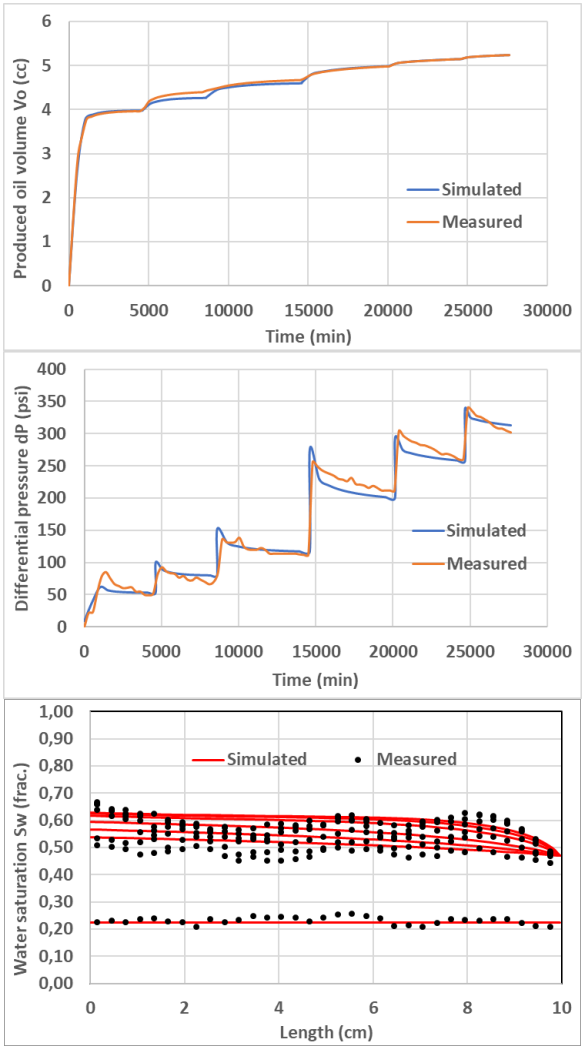


**Fig. 17.** Comparisons between measured properties and numerical simulations for the SD waterflood

Figure 17 represents the results of the produced oil Vo, differential pressure and saturation profiles history matches by tuning the Kro parameter during the simulations. As a matter of fact, local and inlet Krw and Pc are directly determined during the experiment. Pc parameters from log(beta) function were also tuned to fit the experimental data points and to find an optimal value of Sw(Pc=0) for improving the history-match results.

The history match appears acceptable for production Vo and differential pressure, but it is less obvious for the saturation profiles. This is mainly the result of the 1D x-ray limitation and the degree of heterogeneity rock. As explained before, using one single point of x-ray acquisition through the diameter at the core inlet does not represent the average water saturation through the inlet corresponding section.

In order to better history-match the production and differential pressure, a modified Corey or L.E.T. function may have been preferred. But in the frame of comparing the SD and SS methods, keeping consistency/coherence and limiting the number of matching parameters, it was decided to keep a Corey model for Kr and provide the best match possible. The resulting Corey parameters were:

Nw=4.5
No=4.0
Krw Max=0.16
Swi=0.224
Sor=0.346

**SS Method:**

In the SS simulations, the SD local Pc was taken as first guess input, preserving the same parameter values discussed earlier but with the value of Sw(Pc=0) adjusted by using saturation profile observations.

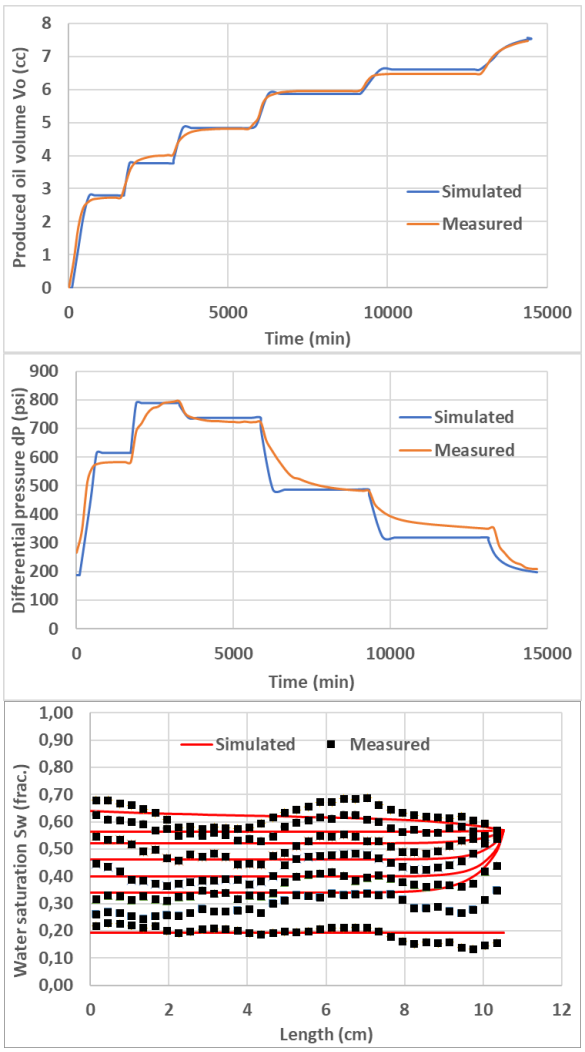


**Fig. 18.** Comparisons between measured properties and numerical simulations for the SS waterflood

As for the SD numerical simulations and history-match, it was difficult to improve the quality of the production and differential pressure history-match results using a simple Corey model. As explained before, even if better results may have been obtained using a modified Corey or L.E.T. function, it was decided to keep consistency/coherence and to limit the number of matching parameters by using a simple Corey model for Kr. The resulting Corey parameters were:

Nw: 3.5
No: 3.0
Krw Max=0.220
Swi=0.193
Sor=0.330

Figure 19 represents both uninterpreted and interpreted SS Kr and Pc curves:

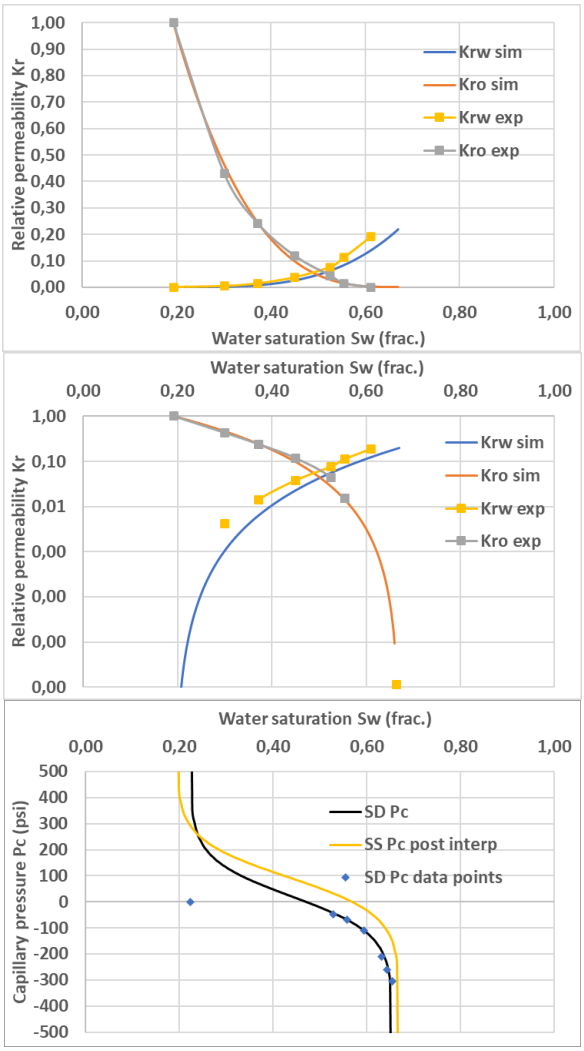


**Fig. 19.** Pre- and post-interpretation Kr and Pc curves for the SS waterflood

Note that Forbes Pc curves as shown in Figure 15 were tested for the two SD and SS waterfloods. An acceptable history-match of dP and Vo were obtained using newly interpreted Kr curves. The observations were:

- The newly interpreted Kr curves were found to be very close to the Kr curves obtained with log(Beta) Pc
- The Forbes Pc function does not mimic the outlet Sw, as shown in saturation profiles in Figure 16 and Figure 17 where a log(Beta) Pc function was used with an appropriate value of Sw(Pc=0).

**Centrifuge Pc Simulation and History-Matching:**

The local centrifuge capillary pressure was obtained using the Forbes' approach (Figure 15). The Kr curve was built with a Corey model, with No equal to 4, as for the single-step test. A first guess of water Corey exponent Nw equal to 2 and Krw Max of 0.2 were tested before running the history-match optimization. The best history match was finally obtained with the below Kr and Pc curves:

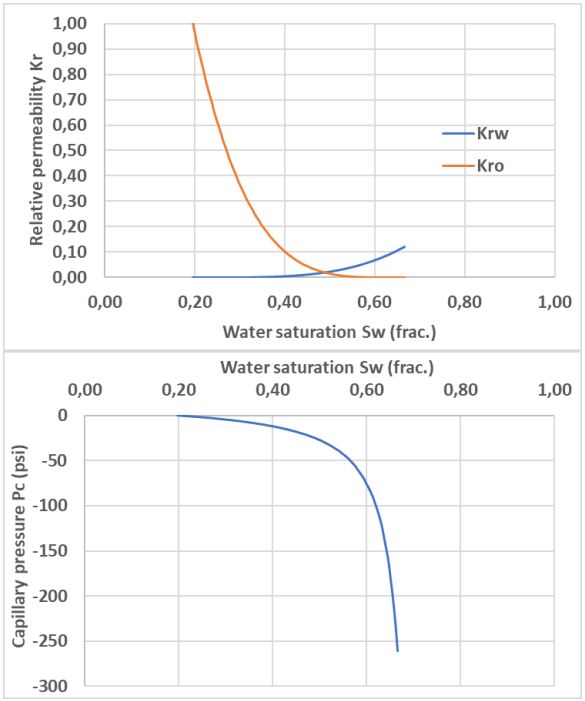


**Fig. 20.** Interpreted Kr curve for the Pc multistep test with the associated Forbes' Pc curve

Nw=3.8
No=4.0
Krw Max=0.12
Swi=0.197
Sor=0.334

The quality of the history-match is presented in Figure 21:

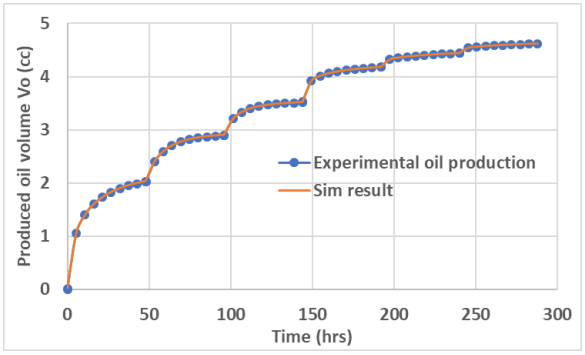


**Fig. 21.** Interpreted Kr curve for the Pc multistep test with the associated Forbes' Pc curve

### Centrifuge Kro Simulation and History-Match:

An history-match of the single-step centrifuge oil production was performed. The Kro was taken as calculated via Hirasaki's method (Figure 16). The same Forbes Pc curve as is in Figure 15 was used as input. An initial Krw guess with Corey exponent Nw equal to 4 was attempted first. Krw Max, Sor and Nw were then tuned for the history-match. Considering the Pc and Kro parameters are well determined, the resulting Kr and Pc curves are shown in Figure 22:

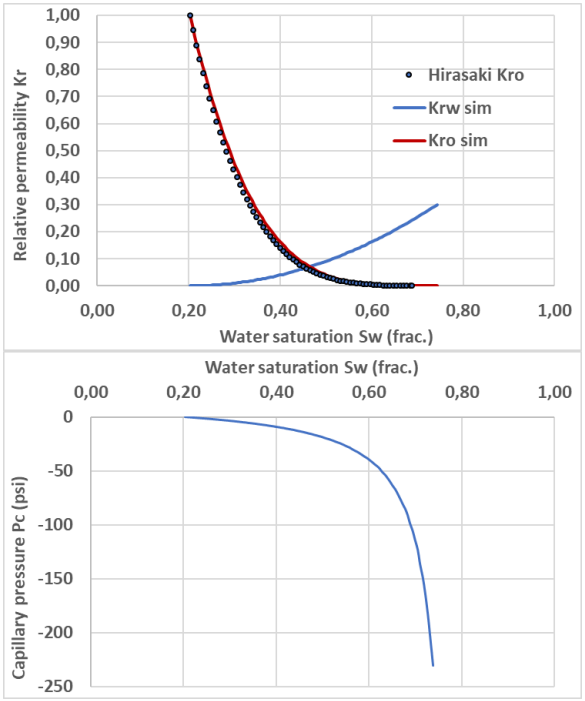


**Fig. 22.** Optimized Kr curve for single-step centrifuge with fixed Forbes Pc

To history-match the oil production Vo, a Corey coefficient of 2 was taken for Nw.

Nw=2
No=4
Krw Max=0.30
Swi=0.203
Sor=0.257

The resulting history-match is shown in Figure 23:

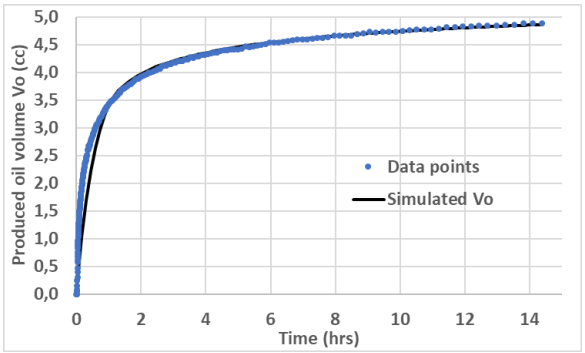


**Fig. 23.** Measured and simulated Vo for the single-step Kr centrifuge test

It is difficult to history-match the early oil production well, probably because no spontaneous displacement was performed before the forced imbibition cycle.

## Kr and Pc Comparisons

### Kr Comparison:

For comparing the petrophysical parameters Kr and Pc from different experiments but on the same rock type, it is generally recommended to plot the results using the same value of Swi (the averaged value) and preserving the recovery information. In this study, the Swi values were

found to be very close. It was decided to directly compare the results without rescaling them to a same value of Swi.

Reminder: for the SD and SS tests, the material balance method was preferred to the x-ray method to interpret the data.

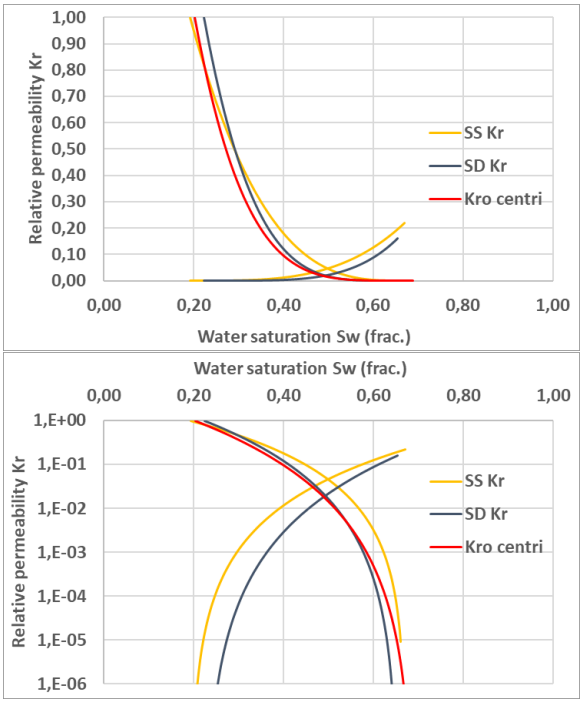


**Fig. 24.** Comparison of SD, SS and centrifuge relative permeability curves

Figure 24 shows that centrifuge and SD Kro curves overlap nicely while SS and SD Kr curves on the Cartesian plot look quite similar. But the semi-log graph better highlights the differences. All can see that SS Kr shows higher oil and water mobility at same saturation compared to the SD. It may be due to the heterogeneity or wettability differences. Fraction flow curve helps in comparing the SD and SS Kr curves:

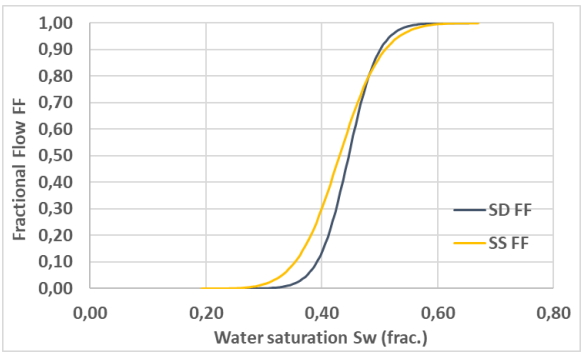


**Fig. 25.** Comparison of relative permeability ratios

Figure 25 shows that the SD case is more optimistic from Swi to Sw~50% while SS case is more optimistic from Sw~50% to residual oil saturation Sor. The difference can be explained by the difference in degree of heterogeneity, the lack of equilibrium during the SD test, as shown on the dP signal in Figure 17, possible effect of the capillary contact between the samples. Wettability difference may also explain the difference despite the tests were run at same conditions, with same fluids, at same Swi and with initial uniform fluid distribution for both stacks.

The Kr Corey exponents and saturation ranges are not so different as presented in Table 5:

**Table 5.** Final Kr Corey parameters and saturation range

| Test | Krw Max | Swi frac. | Sor frac. | Nw | No |
|---|---|---|---|---|---|
| SD | 0.16 | 0.223 | 0.346 | 4.5 | 4.0 |
| SS | 0.22 | 0.193 | 0.330 | 3.5 | 3.0 |
| Pc centri | 0.12 | 0.197 | 0.334 | 3.8 | 4.0 |
| Kr centri | 0.30 | 0.203 | 0.257 | 2.0 | 4.0 |

Wettability could have also explained the Kr difference, but the parameters in Table 5 highlight an intermediate-wet state of the rocks (typically with 3<Nw<5 and 3<No<6), also confirmed by the positions of the Kr cross-points.

Even if it is not observed on the saturation profiles (Figure 6 and Figure 12), a poor capillary contact could lead to non-uniform fluid distribution and so, lead to a difference in flow behaviour. The use of composite stack may not be a good way to perform the waterflooding tests.

Finally, the use of Pc curve for the SS optimization process/history-match, fixed with same SD Pc parameters may also explain the discrepancy. If porous plate or centrifuge Pc could have been individually performed on the composite core plugs prior the SS test, an averaging process (J-function…) would have been necessary to build an averaged Pc curve, introducing again an uncertainty.

It is concluded that having both Kr and Pc measured during similar test on a non-composite stack (to avoid capillary contact issue), is the most acceptable way of avoiding erroneous interpretation.

Even if it is not an objective of the study, the SD and SS Kr curves were compared to the interpreted Kr curves from the single and multistep centrifuge tests:

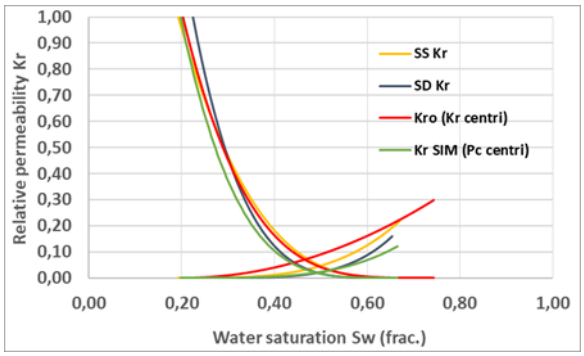

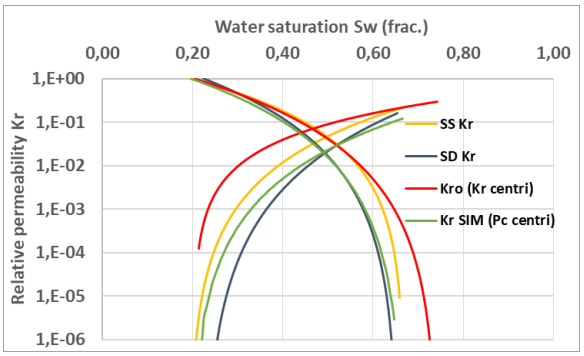


**Fig. 26.** All interpreted Kr curves from coreflooding and centrifuge tests

The Kr curves obtained from the different methods are not so different, except the one from the single-step Kr centrifuge test, probably due to the small amount of signal/data to be history-matched and re-use of the multistep Pc sample after cleaning it again, restored wettability being maybe different. Other curves are in the same range of saturation, close Kr cross-points, close Krw Max and close Kr curvatures, showing a certain consistency in the obtained results. In reservoir engineering, it is not unusual to observe such Kr envelops when dealing with a same rock type.

**Pc Comparison:**

Both the local Pc from centrifuge obtained using the Forbes approach and local Pc directly obtained from SD method are plotted together:

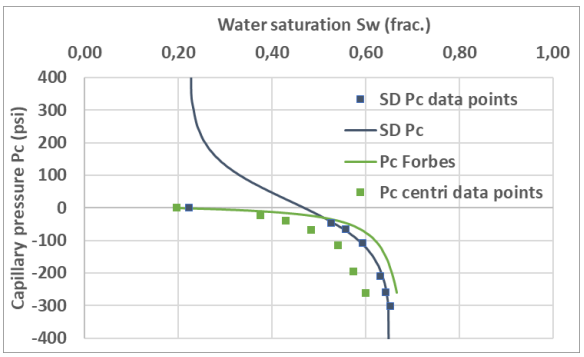


**Fig. 27.** SD and SS capillary pressure Pc curves

Despite using oil at different conditions (dead oil for centrifuge – live oil for SD), Figure 27 shows an acceptable similarity between the SD and Forbes Pc curves. It is very encouraging to notice that the SD method provides similar local Pc to the Forbes method using centrifuge. Again, the SD Sw was analytically calculated and not obtained using the 1D x-ray method. Also, note that there was no spontaneous imbibition performed before running the forced centrifuge and SD imbibition tests. It could have helped in validating the SD Pc, especially the Sw value at Pc=0.

Figure 28 shows all measured and interpreted Pc curves. The interpreted negative Pc parts are all close together, proving a certain consistency of the results and adequate interpretation workflow. The positive part of the Pc curve was unfortunately not measured. It could have been done using the semi-dynamic method.

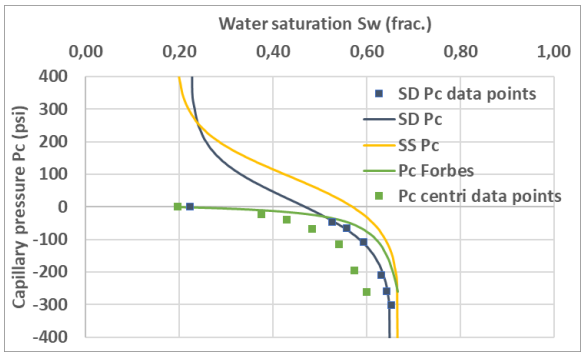


**Fig. 28.** Capillary pressure Pc curves

Based on the capillary pressure curves, it is observed that the SS stack behaves as a more water-wet rock than the SD stack, which is consistent with the observation on the fractional flow (Figure 25). Further investigations must be done to better understand the potential wettability change during the forced imbibition using different methods.

## 6 Conclusions

In this study, several methods for measuring relative permeability and capillary pressure were tested in order to compare the data results and validate the SD method as a unique experiment able to provide both petrophysical parameters during a same test, on same core, with live fluids at real reservoir conditions. It was concluded that:

- The SD Pc data points were found to be similar to the local analytical Forbes Pc obtained during the multistep centrifuge, despite aging and testing with two different oils (dead versus live). The interpreted SD Pc curve using the log(Beta) function passing through the data points is also forced to pass on the true value of Sw(Pc=0) observed on the saturation profiles. Unfortunately, neither the positive part of SD Pc nor the spontaneous imbibition displacement prior centrifuge test were acquired in this study

- The SD Kr was quite different from the SS one. Assuming that the wettability was identical in both tests, the difference may be explained by the rock heterogeneity. The interpreted SS Kr curve was obtained using SD Pc curve (and using centrifuge Pc curve, not presented here), while SD Kr and Pc curves are directly measured during the same test on same composite stack. This is a real advantage to avoid erroneous interpretation

- The simulated SD Kro was consistent with centrifuge Kro. This observation is very encouraging, validating the workflow for the SD history-matching process

- Large rocks should be preferred to composite stacks to avoid potential capillary contact issue

- The quality of the simulated and interpreted Kr curves from the centrifuge tests (multistep and single step) are more questionable because they are based on oil production history match only

If the results of the study are building confidence in the semi-dynamic approach to determine both relative permeability and capillary pressure, some experimental improvements are still required:

- 2D or even 3D x-ray method should be preferred to the 1D or analytical means to measure the inlet water saturation, especially for heterogeneous rocks. A new x-ray setup is being tested in TOTAL [11]. This system allows having enough contrast between water and oil without additional dopants, reducing the risk of a wettability change during the waterfloods

- Pc curve, including the positive part, must be measured with the SD method to determine the full Pc and to better quantify the value of Sw(Pc=0). This can easily be done with the current SD setup, by reducing the oil flow rate and recirculating water at the outlet before injecting water

- The conclusions of this study would need to be confirmed by performing more tests and ensuring the repeatability of the observed results

- Wettability alteration, from the initial restoration while recirculating oil at the core outlet during the semi-dynamic test or while co-injecting oil during the steady-state test, both in a closed loop, requires more attention and investigation

- Finally, a large project for multiple history-matching process is ongoing at TOTAL with the aim of finding Kr and Pc curves via simultaneous assisted history-match on data collected from several experiments [12]

The authors would like to thank TOTAL and Schlumberger for permission to publish this work.

## Nomenclature

*A: section area, in $cm^2$*
*CT: Computed Tomography*
*dP: differential pressure, in psi*
*HPHT: High Pressure High Temperature*
*ISSM: in situ saturation monitoring*
*Kg: apparent gas permeability, in mD*
*Kw: water permeability, in mD*
*Keo: oil relative permeability, in mD*
*Kr: relative permeability*
*Krw: relative permeability to water*
*Kro: relative permeability to oil*
*Krw Max: maximum water relative permeability*
*MB: Material Balance*
*MICP: mercury injection capillary pressure*
*NCS: net confining stress, in psi*
*Nw: water Corey exponent*
*No: oil Corey exponent*
*Pc: capillary pressure, in psi*
*Pp: pore pressure, in psi*
*Pconf: confining pressure, in psi*
*Pi: inlet pressure, in psi*
*Po: outlet pressure, in psi*
*Qw: water flow rate, in cc/min*
*Qo: oil flow rate, in cc/min*
*ROS: Remaining Oil Saturation*
*SD: Semi-Dynamic method*
*SS: Steady-State method*
*SEM: Scanning Electron Microscopy*
*So: oil saturation, in v/v or %*
*Sor: residual oil saturation, in v/v or %*
*<So>: average of oil saturation, in v/v or %*
*Sw: water saturation, in v/v or %*
*Swi: irreducible water saturation, in v/v or %*
*<Sw>: average of water saturation, in v/v or %*
*<$Sw_{sep}$>: average of water saturation using separator, in v/v or %*
*<$Sw_{x\text{-}ray}$>: average of water saturation using x-ray attenuation method, in v/v or %*
*S*: normalized water saturation, in v/v or %*
*T°C: temperature, in °C*
*TS: Thin Section*
*USS: Unsteady-State method*
*Vo: produced oil volume*
*XRD: X-Ray Diffraction*
*X-Swi: irreducible water saturation measured with x-ray attenuation method, in v/v or %*

*$\phi_{He}$: helium porosity, in v/v or %*
*$\rho_w$: water density, in g/cc*
*$\rho_o$: oil density, in g/cc*
*$\mu_w$: water viscosity, in cP*
*$\mu_o$: oil viscosity, in cP*

## References

1. T.S. Ramakrishnan, A. Cappiello, Chem. Eng. Sci., **46** (1991)
2. R. Lenormand, A. Eisenzimmer, Society of Core Analysts, SCA1993-22 (1993)
3. R. Lenormand, P. Schmitz, Society of Core Analysts, SCA1997-17 (1997)
4. J-M. Lombard, P. Egermann, R. Lenormand, Society of Core Analysts, SCA2002-09 (2002)
5. J-M. Lombard *et al.*, Society of Core Analysts, SCA2004-32 (2004)
6. D.R. Maloney, Society of Core Analysts, SCA2006-05 (2006)
7. M.C. Spearing *et al.*, ADIPEC, SPE-171892 (2014)
8. F. Pairoys, Society of Core Analysts, SCA2014-05 (2014)
9. G.J. Hirasaki *et al.*, SPE Reservoir Engineering, SPE-25290 (1992)
10. G.J. Hirasaki *et al.*, SPE Advanced Technology Series, **3**, SPE-24879 (1995)
11. G. Puyou *et al.*, Society of Core Analysts, SCA2017-37 (2017)
12. A.E. Sylte, Society of Core Analysts, SCA2004-17 (2004)